

Quantum Hall Effect at a Four-Terminal Junction

D. G. Ravenhall, H. W. Wyld, and R. L. Schult

Department of Physics, University of Illinois at Urbana-Champaign, 1110 West Green Street, Urbana, Illinois 61801
(Received 23 January 1989)

A quantum-mechanical calculation is made of charged-particle motion at a four-terminal junction of narrow wires in the presence of a magnetic field of arbitrary strength. The scattering probabilities strongly reflect the influence of quantum effects of the junction, including subband thresholds and virtual resonant states. The Hall resistance calculated from them may depart considerably from the classic wide-wire result. Physical features are related to the emergence of pinned Landau levels as the field strength increases.

PACS numbers: 72.15.Gd, 73.20.Dx, 73.50.Jt

The physics of quantum wires, devices made to conduct along two-dimensional surfaces shaped into very narrow channels, is a topic of considerable current experimental¹⁻⁵ and theoretical⁶⁻¹⁰ interest. The quantum Hall effect, observed when such devices are placed in a magnetic field perpendicular to the plane, is modified (compared with the classic wide-sample case)¹¹ by the quantum interference effects that such narrow channels can exhibit. The simplest such device is the four-terminal junction (Fig. 1). Measurement of the voltage across arms III and IV when a current flows from arm I to arm II yields the Hall resistance R_H of the junction.^{6,7} The finite width w of the wires results in a transverse quantization, so that electrons populate subbands whose threshold energies depend on w and on B , the strength of the magnetic field. For large w , and a Fermi energy and B such that n_0 subbands are open, one expects that $R_H = h/e^2 n_0$.¹¹ For small w , however, the experimental results deviate from this prediction.¹⁻⁵ Attempts to understand these deviations have been made by Peeters⁷ and by Büttiker.⁹ An approximation integral to Peeters' work⁷ is the separation of the incident wire from the cross wires by a fictitious potential, and the assumption of barrier leakage to generate the wave functions in the cross wires (weak coupling). As in the zero- B case,⁸ the two-dimensional nature of the junction introduces effects which such a treatment can miss. Büttiker⁹ employs an R -matrix approach which postulates effects (reflection and resonances) induced by the junction which the treatment we now describe yields automatically.

We present an exact quantum-mechanical treatment of the square-well four-terminal junction in the ballistic approximation. (Discussion of the uncertainties introduced by such a treatment has been given recently by Büttiker.¹⁰) With the results of such a treatment, departures from the expected $R_H = h/e^2 n_0$ that arise experimentally can be examined without unnecessary theoretical assumptions. Such a treatment predicts,⁸ for zero B field, bound states at the junction, and also rapid variations with energy of the scattering probabilities (the quantities which in the ballistic approximation determine

R_H) at the thresholds for the opening of new channels (subbands). This complexity is enhanced by the presence of a magnetic field. New structures are found at certain energies, causing R_H to go through zero there. These structures are associated with virtual or resonant states, pinned to the junction, which will become two-dimensional Landau levels in the limit of large B .

As with earlier discussions,^{7,8} we neglect electron-electron and electron-impurity interactions (the ballistic approximation), and we assume for simplicity that the wires are defined transversely by an infinite square well. (For nonzero B the latter assumption does not present a big computational advantage and it can be dispensed with fairly easily.) The method we used earlier for the zero- B case⁸ is extended here to the case of a magnetic field of arbitrary strength. It consists of matching, on the periphery of the square defining the intersection (the dashed lines in Fig. 1), functions which solve the single-wire problem. In the symmetric gauge $\mathbf{A} = (-By/2, Bx/2, 0)$, the analysis outlined in Ref. 8 for the scattering case can be taken over directly, with the replacement of the $B=0$ transverse functions $\sin(n\pi x/w)$ with the appropriate transverse functions $f_n(x/w) \exp(ixy/2l^2)$, where $1/l^2 = qB/\hbar c$ (assumed > 0) defines the magnetic length l . The functions $f_n(x/w)$ are real for waves

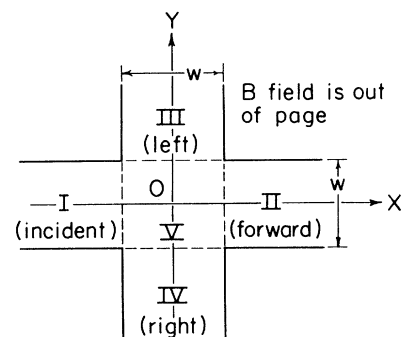


FIG. 1. The four-point junction and the regions I-V referred to in the text.

which propagate along the wire, and were used by Peeters⁷ in his study of the weakly coupled cross wire. They are complex for those waves which decay along the wire. Both types are needed to represent the exact wave function in the arms near the junction. The wave function in the junction (region V, inside the square in Fig. 1) can be thought of as the superposition of a function Ψ_{vert} which vanishes on the boundaries between regions V and I and regions V and II, and Ψ_{horiz} which vanishes on the boundaries between regions V and III and regions V and IV. Ψ_{vert} is then expanded in the same set of wave functions used in regions III and IV, while Ψ_{horiz} is expanded in the set used in regions I and II. The full wave function in region V is then a superposition of all such types of wave functions, both propagating and evanescent, from both horizontal and vertical arms. We compute them by using a numerical solution of the Schrödinger equation. A full description will be given elsewhere.¹²

As in the zero- \mathcal{B} case, matching the wave functions and their normal derivatives at the edges of the square produces eight equations (two for each edge). Approximating the various wave functions by expansions with M transverse functions (n_0 open or propagating modes and $M - n_0$ closed or evanescent modes) leads to an $8M \times 8M$ matrix whose inverse yields the scattering or S matrix. This scattering matrix expresses the outgoing waves in terms of the incoming waves, and one immediately obtains the probabilities for scattering from incident open channel n to final open channel n' forwards ($f_{nn'}$), sideways to the right ($s_{Rnn'}$), sideways to the left ($s_{Lnn'}$), and backwards by reflection ($r_{nn'}$). The general analysis of Büttiker⁶ then gives the Hall resistance R_H as a function of the total probabilities $F = \sum_{nn'} f_{nn'}$, $S_R = \sum_{nn'} s_{Rnn'}$, $S_L = \sum_{nn'} s_{Lnn'}$, and $R = \sum_{nn'} r_{nn'}$, summed over all open channels,

$$\mathcal{R} = \frac{e^2}{h} R_H = \frac{2(S_R - S_L)}{(2F + S_R + S_L)^2 + (S_R - S_L)^2}.$$

It is noteworthy that the unitarity property, which limits the original probabilities by the relationship

$$\sum_{n'} (r_{nn'} + f_{nn'} + s_{Rnn'} + s_{Lnn'}) = 1,$$

and which therefore limits the total quantities by $R + F + S_R + S_L = n_0$, the number of open channels, does not restrict \mathcal{R} to be $1/n_0$, the expected large- w result. The plateau with this value of \mathcal{R} corresponds to $S_R = n_0$ and all the other probabilities being zero, but unitarity certainly does not require those values. For physically accessible values of the scattering probabilities, \mathcal{R} may be larger or smaller than $1/n_0$, and it may even be negative (see also Ref. 9). These departures are the consequence of quantum effects associated with the junction, and they constitute the new results that we present.

Figure 2 shows the surface \mathcal{R} as a function of kw and $\mathcal{B} = w^2/l^2 = (w^2q/\hbar c)\mathcal{B}$. The expected plateaus, of

heights $1/n_0$, are clearly seen at larger \mathcal{B} . They arise in a well-understood way¹¹ as a consequence of the number n_0 of filled bands and the one-dimensional density of states at the Fermi surface. They are bounded by the band edges, whose kw increases with \mathcal{B} . There is also, however, a rich structure of valleys and ridges in the foothills of the plateaus. These are a consequence of the quantum mechanics of the junction. To understand how this comes about, we consider the simpler situation of fixed \mathcal{B} .

The behavior of \mathcal{R} as a function of kw for $\mathcal{B} = 6.0$ is shown in Fig. 3(a). Except at small kw , it bears only a qualitative resemblance to the function $1/n_0$, which is also shown. Figure 3(b) gives the scattering probabilities F , S_R , and S_L which produce it. The pronounced structure of \mathcal{R} is seen to be related in part to the opening of new bands, at $kw \cong 6.48, 9.57, \text{ and } 12.68$, but there are zeros of \mathcal{R} that appear systematically some distance below the first two of those thresholds, and a remnant of structure below the third.

As with any such scattering problem, rapid variations in the partial cross sections (probabilities F , S_R , and S_L) may be associated with virtual levels (resonant states) of the system. To enumerate the possibilities, which depend on the strength of the magnetic field, we recall⁸ that for $\mathcal{B} = 0$ there are two bound states at the junction, trapped by having too low an energy to propagate out through the arms. These are the ground state at $kw \approx 2.56$, which has even parities in both the x and the y directions, and the first excited state at $kw \approx 6.06$, which has odd parities. Relevant to the high- \mathcal{B} limit are the two-dimensional Landau orbits in which the electron is bound by the magnetic field in localized states. They have wave functions $\phi_{nm}(r, \theta) = \chi_{nm}(r) \exp(im\theta)$, where the function $\chi_{nm}(r)$ has $n - 1$ radial nodes, and energy

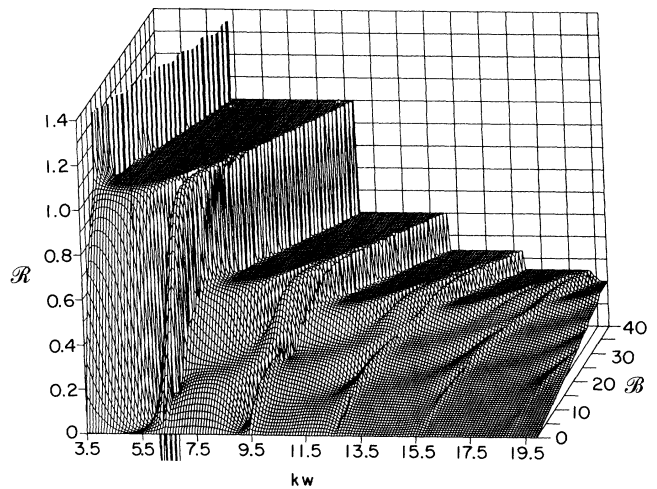


FIG. 2. The dimensionless Hall resistance $\mathcal{R} = (e^2/h)R_H$ as a function of kw ($E_F = \hbar^2 k^2/2m$) and the dimensionless magnetic field $\mathcal{B} = w^2/l^2$.

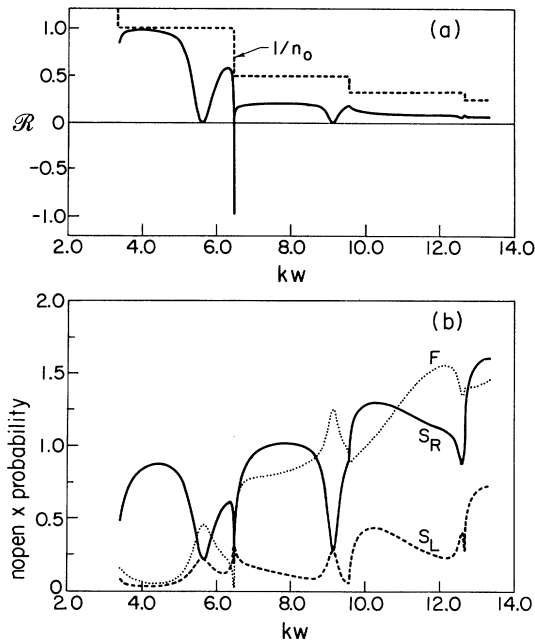


FIG. 3. (a) The dimensionless Hall resistance $\mathcal{R} = (e^2/h)R_H$ as a function of kw ($E_F = \hbar^2 k^2/2m$) for a dimensionless magnetic field $\mathcal{B} = 6.0$. (b) The scattering probabilities F (forward), S_R (right), and S_L (left) as functions of kw for $\mathcal{B} = 6.0$.

levels such that $(kw)^2 = (2n - 1 + |m| - m)\mathcal{B}$. The levels possess discrete degeneracies, for example, that for all $m \geq 0$. Our present interest is in the region of \mathcal{B} lying between these two limits.

For general values of \mathcal{B} , the Hamiltonian is invariant under rotation through $\pi/2$ in the x - y plane, $R(\pi/2)$. Since four such rotations in sequence produce the identity operation, states can be divided into four symmetry classes such that $R(\pi/2)\Psi(x, y) = \Psi(y, -x) = \lambda\Psi(x, y)$ with $\lambda^4 = 1$, i.e., $\lambda = 1, -1, i, \text{ or } -i$. The scattering states described earlier can be decomposed into these symmetry classes, each with a phase shift δ_λ (or phase shifts, for $n_0 \geq 2$). Rapid variations with kw of the probabilities can be associated with rapid changes in one or the other of these phase shifts, and such behavior may then indicate the presence of a virtual quasibound state with that same symmetry, as a pole in the scattering matrix at a nearby complex value of kw . These poles are searched for by repeating the whole calculation for complex values of kw . The zero- \mathcal{B} ground state possesses the symmetry $\lambda = 1$. It remains a stable state below the lowest band edge for all \mathcal{B} , and for large \mathcal{B} becomes the nodeless Landau level $n=1, m=0$, as is verified by examining its spatial wave function $\Psi(x, y)$. In the present non-interacting-electron phase of our calculation it has no effect on \mathcal{R} . The zero- \mathcal{B} first excited state, which belongs to $\lambda = -1$, acquires a finite width when \mathcal{B} is not zero; i.e., at its pole, kw has a negative imaginary part.

As \mathcal{B} increases its width increases, and $\text{Re}(kw)$ grows faster than the kw of the second band edge, which it crosses when $\mathcal{B} \sim 6$. The negative values of \mathcal{R} at $kw \approx 6.5$ in Fig. 3(b) are produced by this virtual state, which at this value of \mathcal{B} occurs close to the second band edge. After crossing the band edge, this state (pole) moves onto an unphysical sheet of the scattering matrix and no longer affects \mathcal{R} .

A finite value of \mathcal{R} requires that left and right scattering have unequal probabilities, and thus must involve the states of $\lambda = i$ and $-i$ symmetry; a zero value of \mathcal{R} then requires that δ_i and δ_{-i} become equal (modulo π), which happens when one of them changes rapidly by an amount comparable to π . The rapid variation of \mathcal{R} that occurs at the values $kw \approx 5.6$ and 9.2 in Fig. 3(a) is associated with virtual states of these symmetries. These states are found to have large widths as $\mathcal{B} \rightarrow 0$ (and thus have little physical effect there) and as \mathcal{B} increases they become narrower. The state responsible for the $kw = 5.6$ structure has $\lambda = -i$, and for large \mathcal{B} (≥ 15) it stays just below the second band edge to become the $n=1, m=-1$ Landau level. The $kw \approx 9.2$ structure is due to a $\lambda = i$ state which approaches the third band edge as \mathcal{B} increases, and crosses behind it (onto an unphysical sheet of the scattering matrix) at $\mathcal{B} \sim 13$. By then it is becoming the $n=1, m=1$ Landau level. It should be possible to locate and identify all of the relevant Landau levels at large \mathcal{B} . It is likely, however, that some of them will be on unphysical sheets, and thus will have no practical consequences. The systematics of this behavior has yet to be clarified.

We can now return to Fig. 2 with an understanding of the origins of some of the lowland structure. The ridge which starts at $kw \sim 6.0$, in the vicinity of the second band edge, has on its low- kw side a flat $\mathcal{R} = 0$ valley, the $n=1, m=-1$ Landau virtual state. A deep, narrow chasm, the result of the $\lambda = -1$ excited state, causes there to be a precipitous descent on the high- kw side of the ridge. As \mathcal{B} increases, these effects gradually moderate, until at $\mathcal{B} \sim 15$ the ridge has merged into the steady rise between the plateaus $\mathcal{R} = \frac{1}{2}$ and 1 . There is a similar valley just below the third band edge, at $kw \sim 9.4$, due to the $n=1, m=1$ Landau level, but only gradual structure on its high- kw side, since there is no level there corresponding to the $\lambda = -1$ excited state.

A feature of Fig. 2 which we remark on without a complete understanding of it is that the plateaus $\mathcal{R} = \frac{1}{5}$ and $\frac{1}{6}$, which have a simple explanation when they appear above the fifth and sixth band edges ($kw \approx 16$ and 19 , respectively), appear to extend to considerably below those kw values for small \mathcal{B} . There is even a trace of the $\mathcal{R} = \frac{1}{5}$ plateau at $kw \sim 7.5$. The system appears to "know about" the higher bands before they are opened. This is presumably a reflection of the fact that the wave functions at the junction do involve all of the channels, including the evanescent ones.

A comparison in detail with particular experiments is

not possible here because each individual device may have rounded channel potentials, rounded corners at the junctions, extra elbows in the arms, or even extra terminals. (For example, six-terminal junctions do not have the same \mathcal{R} as the four-terminal junctions because of interference effects.¹²) We can, however, comment in a general way on the relevance to experiments of certain features of Fig. 2. It seems likely that the broad valley where \mathcal{R} goes to zero near $kw=5$ (or at $kw=5.8$ in Fig. 3), and less pronounced valleys elsewhere, have great relevance to the experimentally observed "quenching" of the Hall effect.^{2,13} The extra $\mathcal{R}=\frac{1}{5}$ and $\frac{1}{6}$, etc., plateaus may well be related to the "last plateau" recently reported by Ford *et al.*¹⁴ We intend to address such questions in a more complete discussion.¹²

In summary, according to non-interacting-electron theory there is a rich structure to the Hall resistance as measured in narrow wires which is related to the quantum mechanics of the four-point junction, and the pinned Landau levels which occur there. Some of this structure may be detectable experimentally. Finer details of the structure will be spread out in energy somewhat by finite-temperature effects, but presumably not the broader features. It is also evident that a Hall-resistance measurement emphasizes the effects of the $\lambda=i$ and $-i$ symmetries. Other measurements, with perhaps more complex geometries, may be appropriate for exploring the other symmetries and their states. There are, of course, effects of a many-body nature, and also complications associated with the solid-state physics,¹⁰ which our treatment has not included. It may be that, as with other Hall-effect manifestations, the results are less susceptible to those complications than one would initially expect. That requires, however, considerably more study.

We are indebted for suggestions and encouragement from S.-J. Chang, R. Landauer, J.-P. Leburton, and M.

Stone. We thank M. Büttiker and F. M. Peeters for prepublication copies of their work. We apologize to the many others working in this area of physics of whose research we are not yet aware. The computations presented in Figs. 2 and 3 were made on the Cray XMP-48 computer at the National Center for Supercomputing Applications, Urbana, Illinois. The research was supported in part by NSF Grants No. PHY84-15064 and No. PHY87-01775.

¹G. Timp, A. M. Chang, P. Mankiewich, R. Behringer, J. E. Cunningham, T. Y. Chang, and R. E. Howard, Phys. Rev. Lett. **59**, 732 (1987).

²M. L. Roukes, A. Scherer, S. J. Allen, Jr., H. G. Craighead, R. M. Ruthen, E. D. Beebe, and J. P. Harbison, Phys. Rev. Lett. **59**, 3011 (1987).

³A. M. Chang, G. Timp, T. Y. Chang, J. E. Cunningham, P. M. Mankiewich, R. E. Behringer, and R. E. Howard, Solid State Commun. **67**, 769 (1988).

⁴C. J. B. Ford, T. J. Thornton, R. Newbury, M. Pepper, H. Ahmed, D. C. Peacock, D. A. Ritchie, J. E. F. Frost, and G. A. C. Jones, Phys. Rev. B **38**, 8518 (1988).

⁵J. A. Simmons, D. C. Tsui, and G. Weimann, Surf. Sci. **196**, 81 (1988).

⁶M. Büttiker, Phys. Rev. Lett. **57**, 1761 (1986).

⁷F. M. Peeters, Phys. Rev. Lett. **61**, 589 (1988).

⁸R. L. Schult, D. G. Ravenhall, and H. W. Wyld, Phys. Rev. B **39**, 5476 (1989).

⁹M. Büttiker, Phys. Rev. B **38**, 12724 (1988).

¹⁰M. Büttiker, Phys. Rev. B **38**, 9375 (1988).

¹¹*The Quantum Hall Effect*, edited by R. R. Prange and S. M. Girvin (Springer-Verlag, New York, 1987).

¹²H. W. Wyld, R. L. Schult, and D. G. Ravenhall (to be published).

¹³We thank J.-P. LeBurton for comments on the significance of this valley.

¹⁴C. J. B. Ford, S. Washburn, M. Büttiker, C. M. Knoedler, and J. M. Hong (to be published).